https://doi.org/10.5194/cp-2020-141
Preprint. Discussion started: 17 November 2020

Climate of the Past Discussions

Holocene climatic changes in the Westerly-Indian Monsoon realm and its anthropogenic impact

Nicole Burdanowitz[1], Tim Rixen[1,2], Birgit Gaye[1], Kay-Christian Emeis[1,3]

[1]Institute for Geology, Universität Hamburg, Bundesstraße 55, 20146 Hamburg, Germany
[2]Leibniz-Zentrum für Marine Tropenforschung (ZMT), Fahrenheitstraße 6, 28359 Bremen, Germany
[3]Institute of Coastal Research, Helmholtz Center Geesthacht, Max-Planck-Straße 1, 21502 Geesthacht, Germany

Correspondence to: Nicole Burdanowitz (nicole.burdanowitz@uni-hamburg.de)

Abstract. The Indian Summer Monsoon (ISM) with its rainfall is the lifeline for people living on the Indian subcontinent today and possibly was the driver of the rise and fall of early agricultural societies in the past. Intensity and position of the ISM have shifted in response to orbitally forced thermal land-ocean contrasts. At the northwestern monsoon margins, interactions between the subtropical westerly jet (STWJ) and the ISM constitute a tipping element in the Earth's climate system, because their non-linear interaction may be a first-order influence on rainfall. We reconstructed marine sea surface temperature (SST), supply of terrestrial material and vegetation changes from a very well-dated sediment core from the northern Arabian Sea to reconstruct the STWJ-ISM interaction. The Holocene record (from 11,000 years) shows a distinct, but gradual, southward displacement of the ISM in the Early to Mid-Holocene, increasingly punctuated by phases of intensified STWJ events that are coeval with interruptions of North Atlantic overturning circulation (Bond events). Effects of the non-linear interactions culminate between 4.6-3 ka BP, marking a climatic transition period during which the ISM shifted southwards and the influence of SWTJ became prominent. The lithogenic input shows an up to 4-fold increase after this time period signaling the strengthened influence of agricultural activities of the Indus civilization with enhanced erosion of soils amplifying the impact of Bond events and adding to the marine sedimentation rates adjacent to the continent.

1 Introduction

Changes in latitude and strength of the ISM were gradual over the course of the Holocene, but were punctuated by distinct climatic events (Herzschuh, 2006). The ISM was strong during the Early Holocene until approximately 6.5 ka ago, and influenced regions farther north than today (Herzschuh, 2006; Prasad and Enzel, 2006). A weakening of the ISM is reflected in many records after the Holocene Optimum Period, commonly attributed to declining summer insolation (Banerji et al., 2020; Herzschuh, 2006), latitudinal insolation gradients (Mohtadi et al., 2016; Ramisch et al., 2016) and feedbacks of climate anomalies such as the Arctic Oscillation (Zhang et al., 2018), the North Atlantic Oscillation (NAO) (Band et al., 2018; Banerji et al., 2020; Kotlia et al., 2015; Lauterbach et al., 2014) or the El Niño Southern Oscillation (ENSO) (Banerji et al., 2020; Prasad et al., 2014; Srivastava et al., 2017).

https://doi.org/10.5194/cp-2020-141
Preprint. Discussion started: 17 November 2020


Climate of the Past Discussions

Changes of the ISM system not only affected hydrological conditions and vegetation in this region, but were also an important constraint on the expansion and dispersal of the Indus civilization, also known as Harappan civilization, emerging around 5 ka ago (Durcan et al., 2019; Giosan et al., 2012, 2018; Possehl, 1997). Growing agricultural activities adjacent the northwestern Arabian Sea increased soil erosion and, therefore, terrigenous sediment input (Gourlan et al., 2020). Further, the decrease of ISM precipitation favored the development of combined summer and winter cropping as well as drought-tolerant crops (Petrie and Bates, 2017). Winter precipitation intensity and interannual variability in the present-day northwestern region of the Indian Monsoon (IM) domain is governed by STWJ-induced events of strong precipitation, so called Western Disturbances (WD) (Anoop et al., 2013; Dimri et al., 2016; Hunt et al., 2018; Leipe et al., 2014; Munz et al., 2017; Zhang et al., 2018). Climatological data show a link between the NAO, the position of the STWJ and the strength of the WD during the winter over northwest India (Yadav et al., 2009). A positive NAO is associated with an intensified STWJ and stronger WD and, thus, above normal winter precipitation in this region (Yadav et al., 2009). The interaction, position and strength of the IM and the STWJ on millennial to Holocene timescales are yet poorly understood, because the pronounced signal of the ISM dominates sedimentary records, and high-quality records in the region where IM and STWJ interact are sparse.

The northeastern (NE) Arabian Sea (AS) is located in the region of interaction of IM and STWJ. Whereas the primary productivity during the warm ISM season is driven by lateral transport of nutrient-rich waters from the Oman upwelling area (Schulz et al., 1996), the NE winds deepen the mixed layer during the colder IWM season due to convective mixing leading to enhanced primary productivity and carbon exports to the deep sea (Banse and McClain, 1986; Madhupratap et al., 1996; Rixen et al., 2019). The NE AS holds high-quality archives due to excellently preserved and highly resolved sediment records deposited on the shelf and slope impinged by a strong oxygen minimum zone (OMZ) between 200 m and 1200 m water depth (von Rad et al., 1995; Schott et al., 1970; Schulz et al., 1996). Most existing records have poor temporal resolution or do not bracket the entire Holocene (Böll et al., 2014, 2015; Giosan et al., 2018; Lückge et al., 2001; Munz et al., 2015), but they outline the interplay of the Indian Winter Monsoon (IWM) with the westerlies in the NE AS realm during the Holocene and suggest that winter monsoon activity intensified between 3.9 and 3.0 ka BP (Giesche et al., 2019; Giosan et al., 2018; Lückge et al., 2001) and intermittently during the last ca. 1.5 ka (Böll et al., 2014; Lückge et al., 2001; Munz et al., 2015).

For a detailed and high-resolution reconstruction, we analyzed lithogenic mass accumulation rates (LIT MAR), alkenone-based SST and *n*-alkane-based land vegetation from the NE AS (Figure 1) over the last 10.7 ka. They document the influence of the IWM and the westerlies on the marine and terrestrial environment in the NE AS region and show that the advent of agriculture in step with climate change significantly enhanced soil erosion.

https://doi.org/10.5194/cp-2020-141
Preprint. Discussion started: 17 November 2020

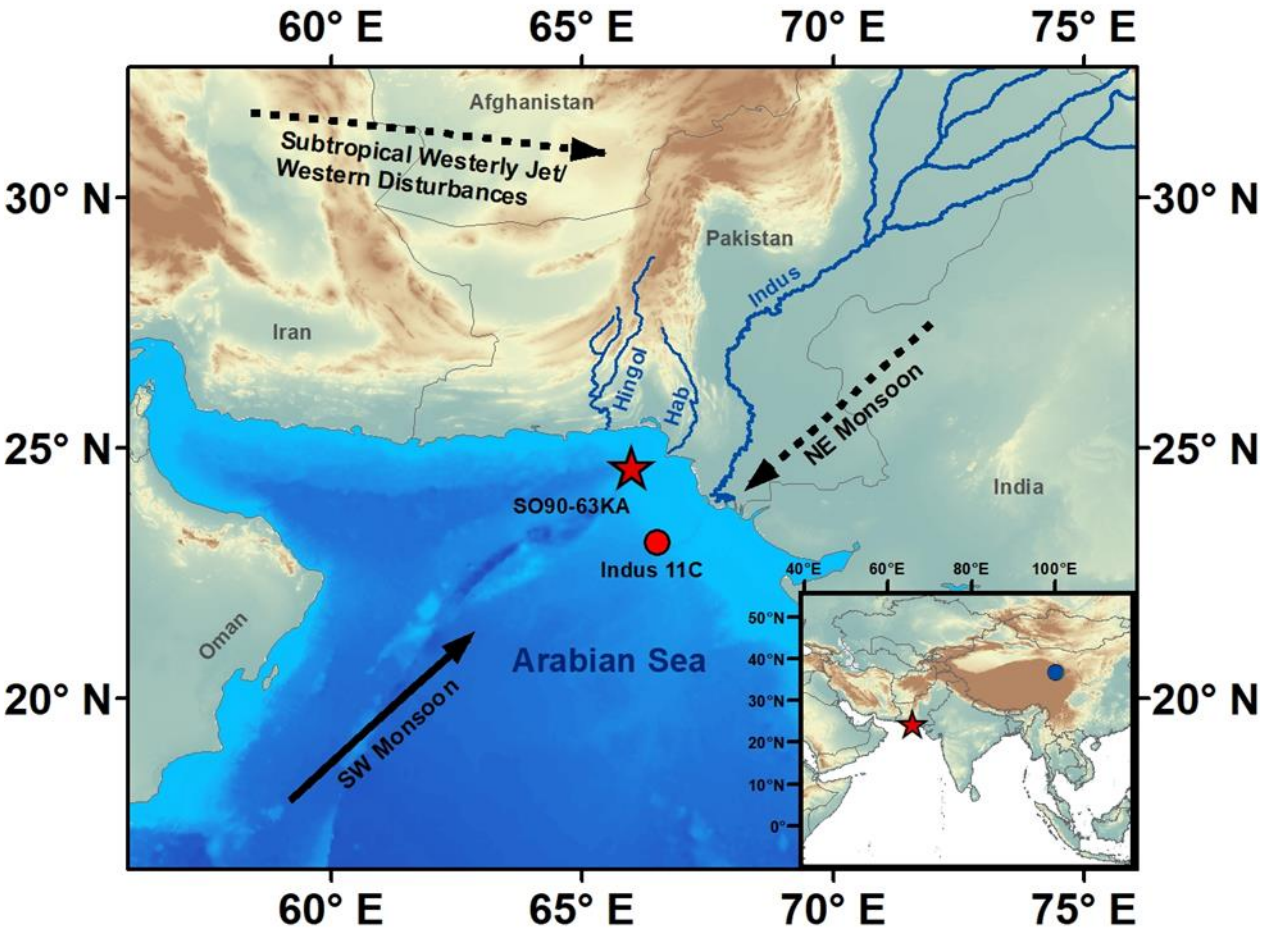

Figure 1: Location of the study site SO90-63KA (red star), the nearby record Indus 11C (Giosan et al., 2018) (red circle) and Lake Qinghai (Hou et al., 2016) (blue circle). The rivers (blue lines) important for the study site are shown. Prevailing wind pattern during the summer monsoon, here indicated as southwest (SW) monsoon is shown with a black arrow. The prevailing wind pattern of the winter monsoon, here indicated as northeast (NE) monsoon as well as the subtropical westerly jet and its induced rain bearing Western Disturbances are shown as black dashed arrows. The map was created using ArcGIS v.10.8 (ESRI, 2019). The bathymetric data are from the General Bathymetric Chart of the Oceans (GEBCO2014; www.gebco.net).

https://doi.org/10.5194/cp-2020-141
Preprint. Discussion started: 17 November 2020

Climate of the Past Discussions

2 Material and Methods

Records presented here were obtained from the box core SO90-63KA (697 cm long), which was retrieved from the Arabian Sea off Pakistan (24°36.6'N, 65°59.0'E, 315 m water depth) during the RV SONNE cruise SO90 in 1993. With the upper 18 cm missing, SO90-63KA covers the last ca. 10.7 ka and encompasses the development of early Bronze Age agricultural societies (Staubwasser et al., 2002, 2003). The chronology is based on 80 ^{14}C dates of planktic foraminifers *Globigerinoides sacculifer* (Staubwasser et al., 2002, 2003) and belongs to the most-well-dated cores from the Arabian Sea. The bulk components, grain sizes and major and trace elements of SO90-63KA were published previously (Burdanowitz et al., 2019; Staubwasser and Sirocko, 2001). We used an extended data set for the grain size analyses of SO90-63KA sediments for the endmember modelling analyses. The procedure is described in the earlier published coarser resolution data set (Burdanowitz et al., 2019).

For the lipid analyses, 2.0 to 13.4 g of freeze-dried and grounded sediment were extracted with a DIONEX Accelerated Solvent Extractor (ASE 200) at 75°C, 1000 psi for 5 min using dichloromethane (DCM) as solvent. The procedure was repeated three times. A known amount of an internal standard (14-heptacosanone, squalane) was added prior to extraction. An additional working sediment standard was extracted for each ASE running sequence. The total lipid extracts (TLEs) were concentrated using rotary evaporation. The TLEs were separated into a hexane-soluble and a hexane-insoluble fraction by Na_2SO_4 column chromatography. The hexane-soluble fractions were saponified at 85°C for 2h using a solution of 5% potassium hydroxide in methanol (MeOH). Afterwards, the neutral fraction was extracted with hexane. Column chromatography using deactivated silica gel (5% H_2O, 60 mesh) was carried out to separate the neutral fraction into an apolar- (containing *n*-alkanes), ketone- (containing alkenones) and polar-fraction by using hexane, DCM and DCM:MeOH (1:1), respectively. The apolar fraction was further cleaned by AgNO3-Si column chromatography using hexane as solvent.

Quantification of the *n*-alkanes and the alkenones was carried out using an Agilent 6850 gas chromatograph (GC) equipped with an Optima1 column (30 m, 0.32 mm, 0.1 µm), split/splitless injector operating at 280°C and a flame ionization detector (FID, 310°C). H_2 was used as carrier gas with a flow of 1.5 ml/min. Samples were injected in hexane and duplicate measurements of each sample were carried out for the alkenones. For the *n*-alkanes, the GC temperature was programmed from 50°C (held 1 min) ramped at 8°C/min to 320°C (held 15 min). An external standard was used for quantification, containing *n*-C_8 to *n*-C_{40} alkanes in known concentration. Repeated analyses of the external standard resulted in a quantification precision of 6 % (1SD).

The average chain length (ACL) of the homologues C_{27}-C_{33} was calculated using following equation:

$$ACL_{27-33} = \frac{27 * C_{27} + 29 * C_{29} + 31 * C_{31} + 33 * C_{33}}{C_{27} + C_{29} + C_{31} + C_{33}}$$

where C_x is the concentration of the *n*-alkane with x carbon atoms.

For the alkenones, the GC temperature was programmed to increase from 50°C (held 1 min) to 230°C at 20°C/min, then at 4.5°C/min to 260°C and at 1.5°C/min to 320°C (held 15 min). The $C_{37:2}$ and $C_{37:3}$ alkenones were identified by comparing the

https://doi.org/10.5194/cp-2020-141
Preprint. Discussion started: 17 November 2020


Climate of the Past Discussions

retention time peaks of the samples and the known working sediment standard. Quantification was carried out by using a known amount of an external standard (14-heptacosanone and hexatriacontane).

We calculated the alkenone unsaturation index using the following equation (Prahl et al., 1988):

$$U_{37}^{k\prime} = \frac{C_{37:2}}{C_{37:2} + C_{37:3}}$$

and using the core top calibration of Indian Ocean sediments (Sonzogni et al., 1997) to convert the UK'37 index to SSTs:

$$SST = \frac{U_{37}^{k\prime} - 0.043}{0.033}$$

For each sample, at least one duplicate measurement was obtained with an average precision of 0.1°C (1SD). The precision of the replicate extractions of the working standard sediment (n=13) and duplicate measurements of each replicate was 0.5°C (1SD).

The total mass accumulation rates (MAR) were calculated by multiplying the dry bulk density (DBD) with the linear sedimentation rate (LSR). The LSR was ascertain by using age model depth and age interval values. DBD was calculated with following equation (Avnimelech et al., 2001):

$$DBD = \frac{weight\ dry\ sample\ (Wd)}{total\ sample\ volume\ (Vt)}$$

with

$$Vt = volume\ of\ solids + volume\ of\ water$$

$$= \frac{weight\ dry\ sample}{particle\ density} + (weight\ wet\ sample - weight\ dry\ sample)$$

For calculating the sediment particle density, we assumed 2.65 g/cm³ for inorganic sediment particles (Blake and Hartge, 1986; Boyd, 1995) and 1 g/cm³ for water density. We performed a density correction for organic matter contents assuming a density of 1.25 g/cm³ for organic particles (Boyd, 1995):

$$sediment\ particle\ density_{weighted\ average} = 1.25 * \%OM + 2.65 * (100 - \%OM)$$

It has to be noted that we did not calculate the LIT MAR between 9.4 and 8.5 ka BP because the core was dried out in this section.

The wavelet power spectrum analyses of LIT MAR were carried out using a Matlab Wavelet script (Torrence and Compo, 1998).

3 Results & Discussion

3.1 Holocene climate change in the NE Arabian Sea realm

Changes in the alkenone producing coccolithopores community *Emiliania huxleyi* and *Gephyrocapsa oceanica* in the NE AS are controlled by changes in the nutrient availability and the mean mixed layer depth (Andruleit et al., 2004). Although, the

https://doi.org/10.5194/cp-2020-141
Preprint. Discussion started: 17 November 2020


Climate of the Past Discussions

coccolithophores community in the NE AS varies over the course of the year with higher alkenone fluxes during winter and spring, Böll et al. (2014) found that the alkenone-based SST reconstruction is representative for annual mean SST. The lithogenic material at the core site is supplied by fluvial input from the Makran rivers (Forke et al., 2019; Lückge et al., 2002; von Rad et al., 2002; Staubwasser and Sirocko, 2001; Stow et al., 2002) and by aeolian input probably from the Sistan Basin region in the border region of Afghanistan and Iran (Burdanowitz et al., 2019; Forke et al., 2019; Kaskaoutis et al., 2014; Rashki et al., 2012). At present dust from the Sistan region is transported to the NE AS by northerly Levar winds during summer and northeasterly and westerly wind during winter (Hussain et al., 2005; Kaskaoutis et al., 2015; Pease et al., 1998; Rashki et al., 2012; Sirocko et al., 1991; Tindale and Pease, 1999).

The SSTs reconstructed from our record range between 25.9 and 27.9°C throughout the Holocene. Waning glacial conditions in the region during the Early Holocene resulted in consistently lower SSTs until ca. 8.7 ka BP in the NE AS (Böll et al., 2015; Gaye et al., 2018; Giosan et al., 2018) (Figure 2). Between 8.7 and 8.1 ka BP SST increased from 26.0°C to 27.2°C and was accompanied by rising LIT MAR around 8.4 to 8.3 ka BP. Coeval rapid changes have been identified across the entire IM realm (Dixit et al., 2014; Rawat et al., 2015) and mark the so-called 8.2 ka event, which was associated with a weakened ISM (Cheng et al., 2009; Dixit et al., 2014). The North Atlantic hematite stained grain (HSG) records indicate eight pronounced cold events, so called Bond events, during the Holocene (Bond et al., 2001). Recent studies suggested that changes in the NAO and the Atlantic Meridional Overturning Circulation (AMOC) might have played an important role and caused at least some of these cold events (Ait Brahim et al., 2019; Goslin et al., 2018; Klus et al., 2018). Whereas some Bond events (0, 1, 5, 7 & 8) occurred during negative NAO-like conditions, linked to a reduction in North Atlantic Deep Water formation, the other Bond events (mainly during the Mid-Holocene) occurred during positive NAO-like conditions (Ait Brahim et al., 2019). The weakened ISM of the 8.2 ka event has been linked to one of these North Atlantic cool phases (Bond event 5) and is interpreted to signal a decrease in ocean heat transport that induced a marked southward shift of the Intertropical Convergence Zone (ITCZ) (Cheng et al., 2009). Although our SST record shows no evidence of the 8.2 ka cold event in the NE AS, $\delta^{18}O$ data of *Globigerinoides ruber* of the same core signal abruptly declining Indus river discharge around 8.4 ka BP (Staubwasser et al., 2002), accompanied by rising LIT MAR indicative for strong soil erosion. It is plausible that this cold event, observed in both the continental records and marine proxies, led to a short southward migration of the ITCZ and drying on the adjacent continent, resulting in a decoupling of the oceanic vs. land proxies in our core. High SSTs prevailed after the Early-Mid Holocene transition at ca. 8.1 ka BP until ca. 5.2 ka BP and are consistent with other Arabian Sea records (Böll et al., 2015; Gaye et al., 2018; Giosan et al., 2018). This warm period encompasses the Mid-Holocene climate optimum period and is characterized by low LIT MAR and increasing fluvial input (Figure 2) due to high precipitation rates in the North Himalayan region (Burdanowitz et al., 2019; Dallmeyer et al., 2013; Herzschuh, 2006) and a dense vegetation cover which lowered soil erosion.

https://doi.org/10.5194/cp-2020-141
Preprint. Discussion started: 17 November 2020

Climate of the Past Discussions

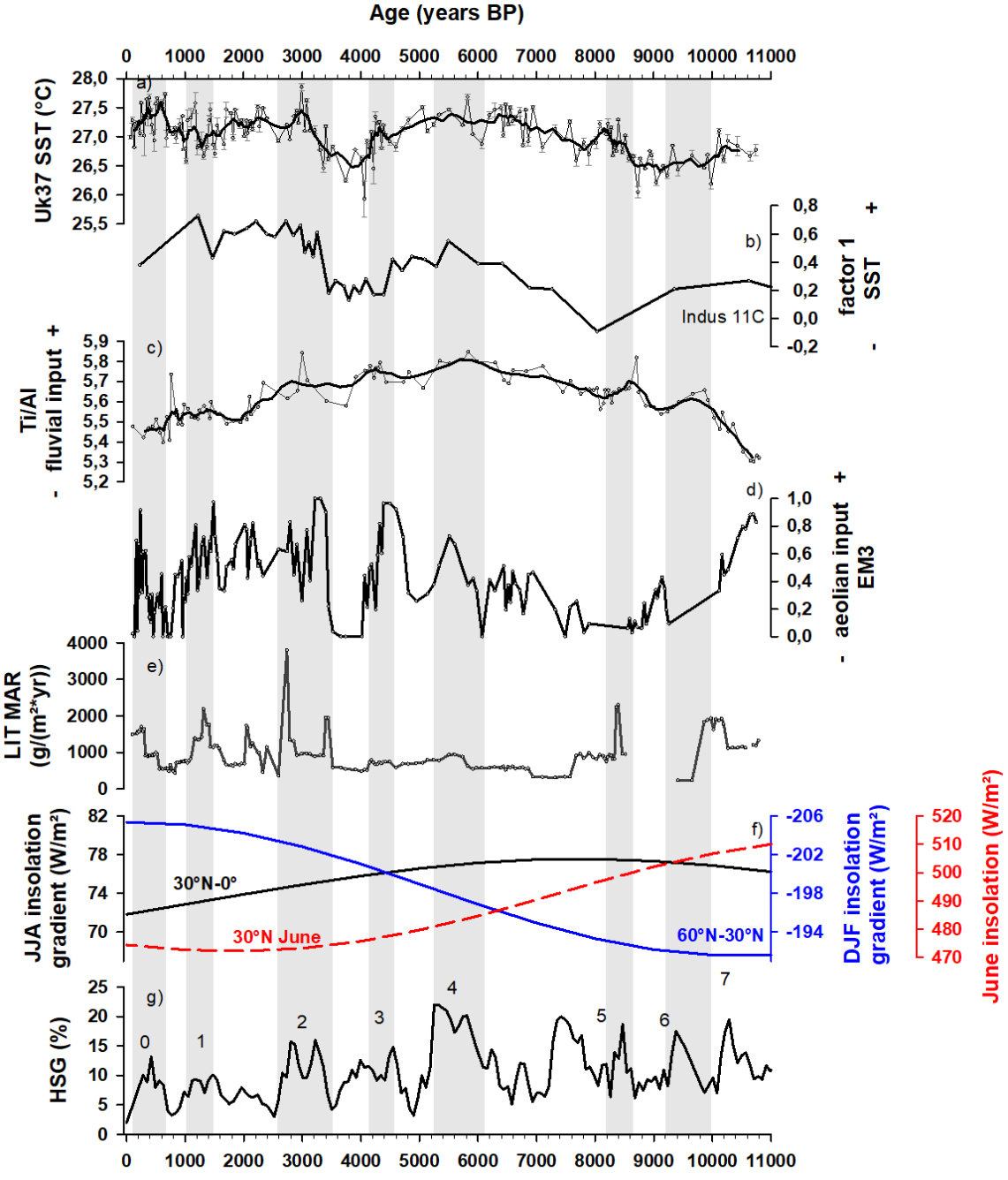

Figure 2: Environmental changes in the NE Arabian Sea. a) alkenone-based reconstructed SST of SO90-63KA, b) factor 1 based on DNA factor analyses of planktic DNA interpreted as SST/winter monsoon indicator 11. c) Ti/Al ratios indicating fluvial input, d) EM3 based on end-member modelling analyses of grain sizes as indicator for aeolian input (Burdanowitz et al., 2019) and e) lithogenic mass accumulation rates (LIT MAR). f) latitudinal insolation gradients (LIG) of summer (JJA: 30°N – 0°, black line) and winter (DJF: 60°N – 30°N, blue line) and summer insolation at 30°N (dashed red line) (Laskar et al., 2004). g) stacked North Atlantic hematite stained grains (HSG) as drift-ice record from core MC52-V29191 with so called "Bond events" (number and grey bars) (Bond et al., 2001). Thick black lines in a) and c) indicates five-point running average.

https://doi.org/10.5194/cp-2020-141
Preprint. Discussion started: 17 November 2020


Climate of the Past Discussions

Thereafter, at about 4.6 ka BP a cooling period occurred which was punctuated by moderate initial cooling event at 4.4 ka BP and a rapid SST decrease of about 1°C between 4.2 and 3.8 ka BP. Foraminiferal analyses of the same core imply lower Indus river discharge and increased IWM mixing between 4.5 – 4.25 ka BP (Giesche et al., 2019; Staubwasser et al., 2003) which coincides with enhanced eolian input (EM3, Figure 2). Giesche et al. (2019) found a weakening of the IWM strength from 4.1 to 3.9 ka BP and a period of cooling between 3.7 and 3.3 ka BP by using salinity sensitive foraminera as proxies. This partly contradicts our SST record. However, the $\delta^{18}O$ record of *G. ruber*, mainly interpreted as a salinity signal, is also affected by water temperature (Giesche et al., 2019; Staubwasser et al., 2003). If the $\delta^{18}O$ signal were interpreted as a temperature rather than a salinity signal, Giesche et al. (2019) argued that the observed increase of the $\delta^{18}O$ around 4.1 ka BP would be consistent with a surface water cooling of about 1°C. This interpretation matches our alkenone-based SST reconstruction at that time. Our record show lower SSTs along with decreasing fluvial input prevailing until 3.0 ka BP. The marked cooling between 4.6 and 3.0 is widespread in the Arabian Sea and on the Indian subcontinent (Gaye et al., 2018; Zhao et al., 2017) and coincides with the rise and fall of the Indus civilization (Wright et al., 2008).

The last ca. 3.0 ka in the record are characterized by high and variable SSTs, LIT MAR, and increasing aeolian inputs, while fluvial inputs of the Makran rivers decrease (Burdanowitz et al., 2019). In contrast to the smoothly decreasing river discharges, the higher SST and especially LIT MAR and aeolian inputs, reveal pronounced variations (Figure 2). These changes are mainly associated with decreasing ISM activity as well as increasing wind in the source areas of the aeolian material and variable IWM strength (Böll et al., 2014, 2015; Burdanowitz et al., 2019; Ivory and Lézine, 2009; Lückge et al., 2001). The main forcing mechanisms have been suggested to be the southward shift of the ITCZ due to decreasing summer solar insolation, thermal land-ocean contrast and/or teleconnection to mid-high-latitude NH climate probably via the STWJ (Böll et al., 2014, 2015; Burdanowitz et al., 2019; Fleitmann et al., 2007; Giosan et al., 2018; Lückge et al., 2001; Mohtadi et al., 2016; Munz et al., 2015, 2017). A stronger impact of NH climate is indicated by high accumulation rated during Bond events 0-2 (Figure 2). The up to 4-fold increase of LIT MAR during the Late Holocene Bond events marks a system shift towards a strong response to mid-high latitude NH climate via the STWJ. This increased precipitation in winter, but decreased precipitation during the summer. Furthermore, this change in the seasonal precipitation pattern enhanced soil erosion due to stronger erosive forces of rivers in largely derelict farmlands exposed to desertification due to an overall increased aridification trend.

3.2 Transition period from low latitudinal to increased mid-high latitudinal influence on the Makran coast

The smooth and long-term decrease of the summer insolation at 30°N after ca. 11 ka BP is an important driver of climate and vegetation changes in the IM and westerlies realm (Fleitmann et al., 2007; Herzschuh, 2006).It is, however, not consistent with the marked cooling event between about 4.6 and 3 ka BP and the subsequent unstable warmer period found in our record. The decreasing summer insolation cannot be the sole driver of these environmental changes even if one considers that the maximum ISM intensity lags the maximum summer insolation by about 3 ka (Ansari and Vink, 2007; Fleitmann et al., 2007; Leipe et al., 2014; Reichart et al., 1998; Zhang et al., 2018; Zhao et al., 2017). A decisive influence instead may be the latitudinal insolation gradient (LIG) that triggers changes of the atmospheric pressure gradient, heat transport and determines the strength and

https://doi.org/10.5194/cp-2020-141
Preprint. Discussion started: 17 November 2020


Climate of the Past Discussions

position of regional atmospheric circulation (Bosmans et al., 2012; Lee and Wang, 2014; Mohtadi et al., 2016; Wang et al., 2017) which has received little attention in paleostudies (Clemens and Prell, 2003). Winter and summer LIG are equally important drivers for the strengths, positions and areal extents of the STWJ and the ISM (Mohtadi et al., 2016; Ramisch et al., 2016). During the winter months (here defined as December – February), the LIG (here defined as the gradient between 60°N-30°N) determines the southernmost position of the STWJ and the frequency of the WDs (Fallah et al., 2017). The LIG (here defined as the gradient between 30°N – equator) during the summer months (here defined as June-August) affects the strength and extension of the ISM over larger timescales (Ramisch et al., 2016). The antagonism and relative magnitudes of the winter and summer LIGs influence the duration of the ISM, as well as STWJ and the frequency of the WDs. Therefore, changes in LIG have probably modulated seasonal length of the IM in the course of the Holocene.

The summer LIG reached its maximum between 8 and 7 ka BP, whereas the winter LIG peaked during the last 1 ka (Figure 2). The net effect of ISM weakening and STWJ strengthening, in combination with dry periods on the adjacent continent to the north, resulted in more frequent dust storms that increased aeolian input to the Arabian Sea during the Late Holocene (Burdanowitz et al., 2019). We suggest that the time period between 4.6 and 3 ka BP marks a transition from an ISM-dominated climate system towards one which is more influenced by the STWJ. This strengthened the teleconnection between the Makran coast and climate variability in the North Atlantic, which is most visible by the link between the LIT MAR record and the Bond events since the end of the time period and associated fall the Indus civilization (Figure 2). A wavelet analysis of LIT MAR data reveals further evidence for the transition period with a change of periodicities between ca 4.2 and 3.5 ka BP (Figure 3). These findings corroborate the hypothesis of a teleconnection between the mid-high-latitude NH climate via the SWTJ and IWM in the NE Arabian Sea region (Böll et al., 2015; Munz et al., 2015, 2017). On a more regional scale, increasing influence of the STWJ coinciding with the transition phase is documented in marine and terrestrial records from the Arabian Sea and Indian subcontinent (Giosan et al., 2018; Hou et al., 2016). Climate simulations for the last 6 ka over Iran have shown a southward shift of the STWJ during the Late Holocene due to increasing winter insolation (Fallah et al., 2017), suggesting a "tipping point" around 3-4 ka BP in the interaction of ISM and STWJ with waxing influence of the STWJ towards the present day. The "tipping point" corresponds to so-called neoglacial anomalies in the Makran region, when a strong winter monsoon and weak interhemispheric temperature contrast (30°N-30°S) were suggested to have been accompanied by a decrease in ISM precipitation (Giosan et al., 2018). Significant temperature oscillations over the last 3 ka were also recorded in the continental record of Lake Qinghai, but are commonly interpreted as an amplified response to volcanic and/or solar forcing (Hou et al., 2016). The manifestation of a meridional shift in STWJ is not restricted to the Arabian Sea region. A southward displacement of the STWJ during the Late Holocene has also been reported from the southern Alps in Europe, the Japan Sea and climate simulations for East Asia (Kong et al., 2017; Nagashima et al., 2013; Wirth et al., 2013), indicating teleconnections on a hemispheric spatial scale.

https://doi.org/10.5194/cp-2020-141
Preprint. Discussion started: 17 November 2020

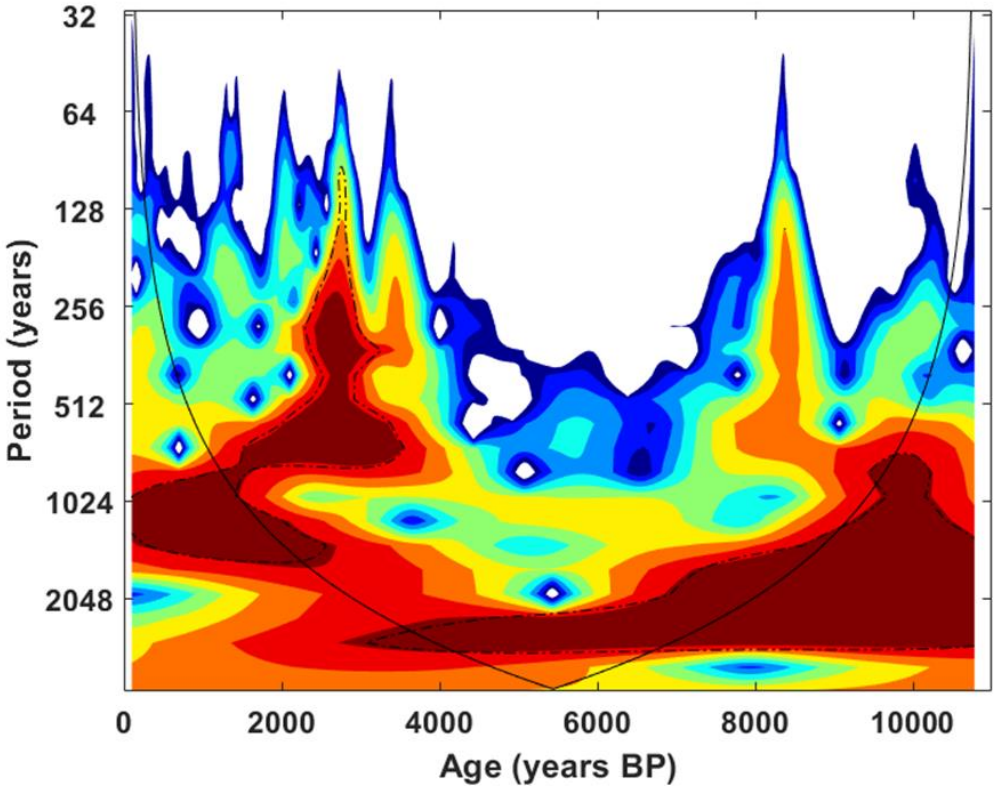

Figure 3: Change of the periodicity in the lithogenic mass accumulation rates (LIT MAR) record. Wavelet power spectrum for LIT MAR of SO90-63KA using a Matlab Wavelet script (Torrence and Compo, 1998). The black line indicates the cone of influence, the dashed black line the 95% significance level. The periodicities change around 3.5 ka and 4.2 ka BP from ca. 2360 years during the Early and Mid-Holocene to ca. 590-710 and 1400 years during the Late Holocene.

Several studies have suggested ENSO as an important driver modulating the climate in the IM realm during the Holocene (Banerji et al., 2020; Munz et al., 2017; Prasad et al., 2014, 2020; Srivastava et al., 2017). In general, an ENSO event is associated with reduced ISM precipitation (Gadgil, 2003). Even though the ENSO events have apparently increased since the last ca. 5000 years (Moy et al., 2002), roughly matching the timing of our observed transition period, we cannot find a correlation of our LIT MAR record with periods of strong ENSO events (not shown). Other studies have shown that the relationship between IM precipitation and ENSO is not linear. Observations (1880 – 2005) suggest that less than half of the severe droughts occurred during El Niño years, while the amount of precipitation was normal or above normal during other El Niño years (Rajeevan and Pai, 2007). A possible reason for this mismatch is the strong effect of the Indian Ocean Dipole (IOD). It can act as an amplifier or suppressor of the ENSO influence in the ISM realm (Ashok et al., 2001, 2004; Behera and Ratnam, 2018; Krishnaswamy et al., 2015; Ummenhofer et al., 2011). A positive IOD can counteract even a strong El Niño forcing leading to "normal" precipitation amounts (Ashok et al., 2004; Krishnaswamy et al., 2015; Ummenhofer et al., 2011). A recent study suggested that a positive IOD shows a tripolar pattern over the IM realm, with above normal precipitation in

https://doi.org/10.5194/cp-2020-141
Preprint. Discussion started: 17 November 2020


Climate of the Past Discussions

central India and below normal precipitation in northern and southern India (Behera and Ratnam, 2018). In contrast, a negative IOD creates a zonal pattern with above normal precipitation in western India and below normal precipitation in eastern India (Behera and Ratnam, 2018). In addition, these authors have linked a positive IOD to warmer SST in the northern AS and vice versa. However, we can only speculate how strong its impact was during the transition period due to the lack of paleorecords reconstructing the IOD.

3.3 The environmental-anthropogenic interaction during the mid-Late Holocene

Widespread anthropogenic land use, such as deforestation or rice irrigation, and associated environmental change is recorded during the Early-Mid Holocene transition period (Petrie et al., 2017; Petrie and Bates, 2017). Especially rice irrigation, starting around 6-4 ka ago, has been suggested to have increased the atmospheric CH_4 concentration since about 5 ka (Figure 4) and thus had a small, but emblematic impact on climate (Ruddiman and Thomson, 2001). The rise of the Indus civilization began around 5.2 ka BP when general aridification decreased river discharges (Giosan et al., 2012). Since ca. 4 ka BP, increasing winter precipitation enabled the development of agriculture along the Indus valley due to less intense floods favoring urbanization (Giosan et al., 2012; Wright et al., 2008). The urban Harappan civilization collapsed towards the end of the climatic transition period when less frequent annual flooding occurred, which was the basis of agriculture. Most of the people migrated from the Indus valley to the Himalaya plains, whereas the remaining society turned into a post-urban society (Clift and Plumb, 2008; Giosan et al., 2012, 2018; Possehl, 1997).

The average chain length (ACL) of plant-wax derived long-chain *n*-alkanes vary in response to vegetation type and/or climatic conditions (Bush and McInerney, 2013; Carr et al., 2014; Meyers and Ishiwatari, 1993; Rao et al., 2011; Vogts et al., 2009). For instance, African savanna plants produce, on average, longer chain *n*-alkanes than rainforest plants (Rommerskirchen et al., 2006; Vogts et al., 2009). In the region of Indus civilization, natural dominated until agriculture proliferated (Giosan et al., 2012) driven by the changing precipitation pattern due to the interplay of the position and strength of the STWJ and ISM (Ansari and Vink, 2007) (Figure 4). During the Mid-Holocene warm period, high SSTs are thought to have fueled the moisture transport to the adjacent continent, which is in line with our SST record (Figure 2). High average summer precipitation and/or more uniformly distributed precipitation during the different seasons favored the development of grasslands in southern Pakistan (Ansari and Vink, 2007; Ivory and Lézine, 2009). This may reflected in a decrease in the ACL of *n*-alkane homologues C_{27} – C_{33} ($ACL_{27\text{-}33}$) between ca. 7 to 5 ka BP (Figure 4). The $ACL_{27\text{-}33}$ increased after the transition period, although the amplitude of $ACL_{27\text{-}33}$ variation is not very high, and decreasing river discharges and increasing aeolian input (Figure 2) indicate prevailing dry conditions after 3 ka BP. It is impossible to separate effects of anthropogenic modified vegetation or climatic driven vegetation changes on $ACL_{27\text{-}33}$ fluctuations s as the $ACL_{27\text{-}33}$ reflects to whole vegetation community. However, but the $ACL_{27\text{-}33}$ increase suggests that humans started to influence the vegetation in the sediment source region and led to the decoupling of the climate signal and the $ACL_{27\text{-}33}$. This is in line with the coeval decoupling of the atmospheric CH_4 concentration and orbitally driven climate changes (Ruddiman and Thomson, 2001). These authors suggested that inefficient early rice farming caused atmospheric CH_4 concentration to increase at around 5 ka BP. Rice agriculture began around 4 ka

https://doi.org/10.5194/cp-2020-141
Preprint. Discussion started: 17 November 2020

Climate of the Past Discussions

BP on the Indian subcontinent and near the Indus River region, adding to the atmospheric CH_4 concentration (Fuller et al., 2011). Further, climatic changes during the Mid-Holocene were suggested to have changed the agricultural system in the region to a "multi-cropping" (summer/winter crops) system (Petrie and Bates, 2017; Wright et al., 2008). This clearly shows that human activities not only modified the vegetation, but also started to impact climate during this time. In a modelling study land cover change associated with prehistoric cultures modified not only local climate, but climate on a broader hemispheric scale via teleconnections (Dallmeyer and Claussen, 2011). Since the transformation of natural into cultivated landscapes favors soil erosion, it is likely that this early human land-use change intensified the impact of the NAO and Bond events on the sedimentation in the NE AS during the late Holocene. The latter in turn documents a clear shift of the climatic system that was associated with the collapse of and deep crises of Late Bronze Age societies in the Mediterranean, Middle East and East Asia.

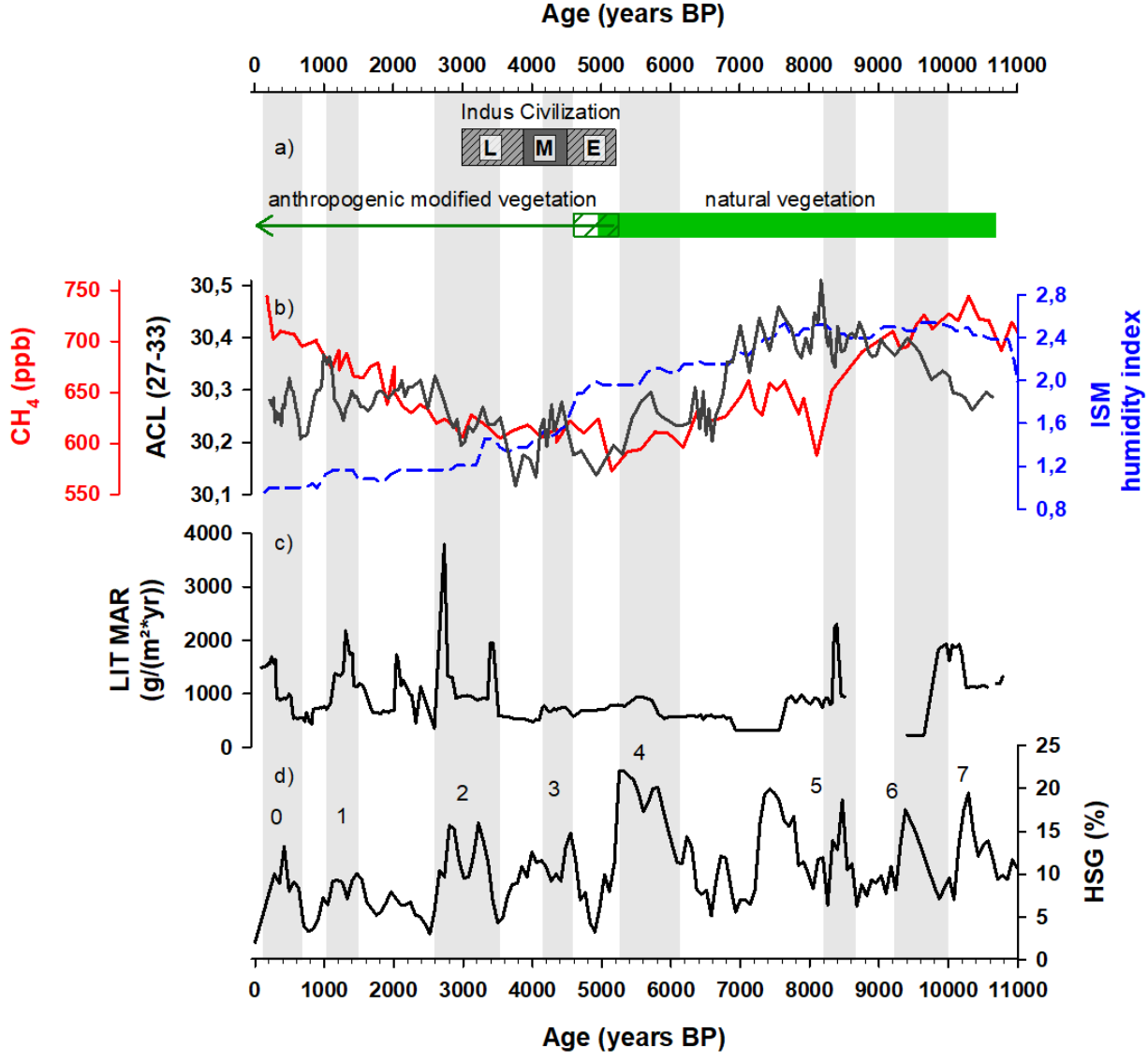

https://doi.org/10.5194/cp-2020-141
Preprint. Discussion started: 17 November 2020

Climate of the Past Discussions

Figure 4: Environmental and anthropogenic interaction. a) different phases of the Indus civilization (Giosan et al., 2012) (L=Late, M=Mature, E=Early) and time periods of our interpreted natural and anthropogenic modified vegetation (green bar and arrow) in comparison to b) average chain length (ACL) of the *n*-alkanes homologues 27-33 (black) and c) LIT MAR of SO90-63KA as well as b) ISM humidity index (Herzschuh, 2006) (blue), CH_4 concentration (red) reconstruction based on Greenland ice cores (Blunier et al., 1995) and d) Bond events (numbers and grey bars) based on the HSG drift-ice record from the North Atlantic (Bond et al., 2001).

The climate transition period between 4.6 and 3 ka BP impacted not only the Indus civilization but also civilizations in Mesopotamia, the Eastern Mediterranean and China (Giosan et al., 2012, 2018; Kaniewski et al., 2013; Liu and Feng, 2012; Wang et al., 2016; Weiss et al., 1993). Today these regions are located slightly north of the northern border of the region influenced by the Asian monsoon (Wang et al., 2016), but where probably within the monsoon realm prior the tranisition period. The series of climatically triggered collapses started at about 4.4 ka in China and reached Mesopotamia and the Eastern Mediterranean between 3.1 and 3.2 ka BP (Giosan et al., 2012, 2018; Kaniewski et al., 2013; Liu and Feng, 2012; Wang et al., 2016). This indicates that this transition period was characterized by a southward shift of the ISM realm, which in combination with socio-economic responses turned into catastrophic changes for Late Bronze Age societies that thrived in the ISM/ STWJ transition zone.

4 Conclusions

Our study of reconstructed SST, LIT MAR and vegetation changes at the Makran coastal region suggests a climatic transition period between 4.6 – 3 ka BP from a low latitude to increased mid-high latitude influence via the STWJ. Prior to this transition period the region was strongly influenced by the ISM and the ITCZ. Our LIT MAR record shows an up to 4-fold increase after the transition period coincident with Bond events in the North Atlantic. We argue that after this period the North Atlantic signals of NAO and Bond events are transmitted to the Makran coast region via the southward shifted STWJ. This supports an earlier modelling study (Fallah et al., 2017) suggesting a southward shift of the STWJ and more winter precipitation near our study area in Iran between 4 and 3 ka BP, which the authors mark as a "tipping point" in that region. Besides a long term drying trend since the Mid-Holocene, this transition period and the associated change in the precipitation pattern (winter vs. summer precipitation) affected the settlements and agriculture of the Indus civilization (Giosan et al., 2012, 2018; Petrie and Bates, 2017). The temporal coincidence gives rise to the hypothesis that humans themselves became environmental drivers prior to the onset of the transition period (Fuller et al., 2011; Ruddiman and Thomson, 2001), instead of only being passive victims of climate change. Whether human impacts suffice to influence the global climate is an ongoing debate, but it is very likely that land cover changes associated with prehistoric cultures modified at least local climate (Dallmeyer and Claussen, 2011). Consequences included a weakened local hydrological cycle that favored desertification, especially in semi-arid regions.

https://doi.org/10.5194/cp-2020-141
Preprint. Discussion started: 17 November 2020

Data availability

The alkenone-based SST, the LIT MAR, the extended grain size used for the EM3 and *n*-alkane data sets of core SO90-63KA will be available at PANGAEA data repository. The previous grain size and elemental data of SO-90KA are available at PANGAEA data repository (https://doi.pangaea.de/10.1594/PANGAEA.900973).

Author contribution

BG and KE designed the study. NB analyzed LIT MAR, alkenones and *n*-alkanes. TR analyzed grain sizes. NB, BG and TR interpreted the data. NB prepared the manuscript with input from all co-authors.

Competing interests.

The authors declare that they have no conflict of interest.

Acknowledgements

We thank F. Langenberg, M. Metzke, C. Staschok, L. Hilbig, L. Meiritz and Y. Akkul for analytical support. S. Beckmann is thanked for the technical support for *n*-alkane and alkenone analyses. We thank an anonymous reviewer of a previous version for comments that helped to improve the manuscript. The study was supported by the German Federal Ministry of Education and Research (BMBF) as part of the CAHOL (Central Asian Holocene Climate, project number 03G0864A), a subproject of the research program CAME II (Central Asia: Climatic Tipping Points & Their Consequences, project number 03G0863G). This study is a contribution to the Cluster of Excellence 'CLICCS - Climate, Climatic Change, and Society', contribution to the Center for Earth System Research and Sustainability (CEN) of Universität Hamburg.

References

Ait Brahim, Y., Wassenburg, J. A., Sha, L., Cruz, F. W., Deininger, M., Sifeddine, A., Bouchaou, L., Spötl, C., Edwards, R. L. and Cheng, H.: North Atlantic Ice-Rafting, Ocean and Atmospheric Circulation During the Holocene: Insights From Western Mediterranean Speleothems, Geophys. Res. Lett., 46(13), 7614–7623, doi:10.1029/2019GL082405, 2019.

Andruleit, H., Rogalla, U. and Stäger, S.: From living communities to fossil assembages: Origin and fate of coccolithophorids in northern Arabian Sea, Micropaleontology, 50, suppl.(1), 5–21, 2004.

Anoop, A., Prasad, S., Krishnan, R., Naumann, R. and Dulski, P.: Intensified monsoon and spatiotemporal changes in precipitation patterns in the NW Himalaya during the early-mid Holocene, Quat. Int., 313(Supplement C), 74–84, doi:https://doi.org/10.1016/j.quaint.2013.08.014, 2013.

https://doi.org/10.5194/cp-2020-141
Preprint. Discussion started: 17 November 2020

345 Ansari, M. H. and Vink, A.: Vegetation history and palaeoclimate of the past 30 kyr in Pakistan as inferred from the palynology of continental margin sediments off the Indus Delta, Rev. Palaeobot. Palynol., 145(3), 201–216, doi:https://doi.org/10.1016/j.revpalbo.2006.10.005, 2007.

Ashok, K., Guan, Z. and Yamagata, T.: Impact of the Indian Ocean dipole on the relationship between the Indian monsoon rainfall and ENSO, Geophys. Res. Lett., 28(23), 4499–4502, doi:10.1029/2001GL013294, 2001.

350 Ashok, K., Guan, Z., Saji, N. H. and Yamagata, T.: Individual and Combined Influences of ENSO and the Indian Ocean Dipole on the Indian Summer Monsoon, J. Clim., 17(16), 3141–3155, doi:10.1175/1520-0442(2004)017<3141:IACIOE>2.0.CO;2, 2004.

Avnimelech, Y., Ritvo, G., Meijer, L. E. and Kochba, M.: Water content, organic carbon and dry bulk density in flooded sediments, Aquac. Eng., 25(1), 25–33, doi:https://doi.org/10.1016/S0144-8609(01)00068-1, 2001.

355 Band, S., Yadava, M. G., Lone, M. A., Shen, C. C., Sree, K. and Ramesh, R.: High-resolution mid-Holocene Indian Summer Monsoon recorded in a stalagmite from the Kotumsar Cave, Central India, Quat. Int., 479, 19–24, doi:10.1016/j.quaint.2018.01.026, 2018.

Banerji, U. S., Arulbalaji, P. and Padmalal, D.: Holocene climate variability and Indian Summer Monsoon: An overview, The Holocene, 1–30, doi:10.1177/0959683619895577, 2020.

360 Banse, K. and McClain, C. R.: Winter blooms of phytoplankton in the Arabian Sea as observed by the Coastal Zone Color Scanner, Mar. Ecol. Prog. Ser., 34, 201–211, doi:10.3354/meps034201, 1986.

Behera, S. K. and Ratnam, J. V.: Quasi-asymmetric response of the Indian summer monsoon rainfall to opposite phases of the IOD, Sci. Rep., 8(1), 123, doi:10.1038/s41598-017-18396-6, 2018.

Blake, G. R. and Hartge, K. H.: Bulk Density, Methods Soil Anal., 363–375, doi:doi:10.2136/sssabookser5.1.2ed.c13, 1986.

365 Blunier, T., Chappellaz, J., Schwander, J., Stauffer, B. and Raynaud, D.: Variations in atmospheric methane concentration during the Holocene epoch, Nature, 374(6517), 46–49, doi:10.1038/374046a0, 1995.

Böll, A., Lückge, A., Munz, P., Forke, S., Schulz, H., Ramaswamy, V., Rixen, T., Gaye, B. and Emeis, K. C.: Late Holocene primary productivity and sea surface temperature variations in the northeastern Arabian Sea: Implications for winter monsoon variability, Paleoceanography, doi:10.1002/2013PA002579, 2014.

370 Böll, A., Schulz, H., Munz, P., Rixen, T., Gaye, B. and Emeis, K. C.: Contrasting sea surface temperature of summer and winter monsoon variability in the northern Arabian Sea over the last 25ka, Palaeogeogr. Palaeoclimatol. Palaeoecol., 426, 10–21, doi:10.1016/j.palaeo.2015.02.036, 2015.

Bond, G., Kromer, B., Beer, J., Muscheler, R., Evans, M. N., Showers, W., Hoffmann, S., Lotti-Bond, R., Hajdas, I. and Bonani, G.: Persistent solar influence on North Atlantic climate during the Holocene., Science, 294, 2130–2136,

375 doi:10.1126/science.1065680, 2001.

Bosmans, J. H. C., Drijfhout, S. S., Tuenter, E., Lourens, L. J., Hilgen, F. J. and Weber, S. L.: Monsoonal response to mid-holocene orbital forcing in a high resolution GCM, Clim. Past, 8(2), 723–740, doi:10.5194/cp-8-723-2012, 2012.

Boyd, C. E.: Bottom Soils, Sediment, and Pond Aquaculture, Springerl., 1995.

https://doi.org/10.5194/cp-2020-141
Preprint. Discussion started: 17 November 2020

Burdanowitz, N., Gaye, B., Hilbig, L., Lahajnar, N., Lückge, A., Rixen, T. and Emeis, K. C.: Holocene monsoon and sea level-related changes of sedimentation in the northeastern Arabian Sea, Deep. Res. Part II Top. Stud. Oceanogr., 166, 6–18, doi:10.1016/j.dsr2.2019.03.003, 2019.

Bush, R. T. and McInerney, F. A.: Leaf wax *n*-alkane distributions in and across modern plants: Implications for paleoecology and chemotaxonomy, Geochim. Cosmochim. Acta, 117, 161–179, doi:10.1016/j.gca.2013.04.016, 2013.

Carr, A. S., Boom, A., Grimes, H. L., Chase, B. M., Meadows, M. E. and Harris, A.: Leaf wax *n*-alkane distributions in arid zone South African flora: Environmental controls, chemotaxonomy and palaeoecological implications, Org. Geochem., 67, 72–84, doi:10.1016/j.orggeochem.2013.12.004, 2014.

Cheng, H., Fleitmann, D., Edwards, R. L., Wang, X., Cruz, F. W., Auler, A. S., Mangini, A., Wang, Y., Kong, X., Burns, S. J. and Matter, A.: Timing and structure of the 8.2 kyr B.P. event inferred from δ18O records of stalagmites from China, Oman, and Brazil, Geology, 37(11), 1007–1010, doi:10.1130/G30126A.1, 2009.

Clemens, S. C. and Prell, W. L.: A 350,000 year summer-monsoon multi-proxy stack from the Owen Ridge, Northern Arabian Sea, Mar. Geol., 201(1–3), 35–51, doi:10.1016/S0025-3227(03)00207-X, 2003.

Clift, P. D. and Plumb, R. A.: The Asian Monsoon: Causes, History and Effects, Cambridge University Press, Cambridge., 2008.

Dallmeyer, A. and Claussen, M.: The influence of land cover change in the Asian monsoon region on present-day and mid-Holocene climate, Biogeosciences, 8(6), 1499–1519, doi:10.5194/bg-8-1499-2011, 2011.

Dallmeyer, A., Claussen, M., Wang, Y. and Herzschuh, U.: Spatial variability of Holocene changes in the annual precipitation pattern: a model-data synthesis for the Asian monsoon region, Clim. Dyn., 40(11–12), 2919–2936, doi:10.1007/s00382-012-1550-6, 2013.

Dimri, A. P., Yasunari, T., Kotlia, B. S., Mohanty, U. C. and Sikka, D. R.: Indian winter monsoon: Present and past, Earth-Science Rev., 163, 297–322, doi:10.1016/j.earscirev.2016.10.008, 2016.

Dixit, Y., Hodell, D. A., Sinha, R. and Petrie, C. A.: Abrupt weakening of the Indian summer monsoon at 8.2 kyr B.P., Earth Planet. Sci. Lett., 391, 16–23, doi:http://dx.doi.org/10.1016/j.epsl.2014.01.026, 2014.

Durcan, J. A., Thomas, D. S. G. G., Gupta, S., Pawar, V., Singh, R. N. and Petrie, C. A.: Holocene landscape dynamics in the Ghaggar-Hakra palaeochannel region at the northern edge of the Thar Desert, northwest India, Quat. Int., 501, 317–327, doi:10.1016/j.quaint.2017.10.012, 2019.

ESRI: ArcGIS Desktop: Release 10.8. Redlands, CA: Environmental Systems Research Institute., 2019.

Fallah, B., Sodoudi, S., Russo, E., Kirchner, I. and Cubasch, U.: Towards modeling the regional rainfall changes over Iran due to the climate forcing of the past 6000 years, Quat. Int., 429(Part B), 119–128, doi:https://doi.org/10.1016/j.quaint.2015.09.061, 2017.

Fleitmann, D., Burns, S. J., Mangini, A., Mudelsee, M., Kramers, J., Villa, I., Neff, U., Al-Subbary, A. A., Buettner, A., Hippler, D. and Matter, A.: Holocene ITCZ and Indian monsoon dynamics recorded in stalagmites from Oman and Yemen (Socotra), Quat. Sci. Rev., 26(1–2), 170–188, doi:10.1016/j.quascirev.2006.04.012, 2007.

https://doi.org/10.5194/cp-2020-141
Preprint. Discussion started: 17 November 2020

Forke, S., Rixen, T., Burdanowitz, N., Ramaswamy, V., Munz, P., Wilhelms-dick, D., Vogt, C., Kasten, S. and Gaye, B.: Sources of laminated sediments in the northeastern Arabian Sea off Pakistan and implications for sediment transport mechanisms during the late Holocene, The Holocene, 29(1), 130–144, doi:10.1177/0959683618804627, 2019.

Fuller, D. Q., van Etten, J., Manning, K., Castillo, C., Kingwell-Banham, E., Weisskopf, A., Qin, L., Sato, Y.-I. and Hijmans, R. J.: The contribution of rice agriculture and livestock pastoralism to prehistoric methane levels: An archaeological assessment, The Holocene, 21(5), 743–759, doi:10.1177/0959683611398052, 2011.

Gadgil, S.: The Indian Monsoon and its variability, Annu. Rev. Earth Planet. Sci., 31(1), 429–467, doi:10.1146/annurev.earth.31.100901.141251, 2003.

Gaye, B., Böll, A., Segschneider, J., Burdanowitz, N., Emeis, K.-C., Ramaswamy, V., Lahajnar, N., Lückge, A. and Rixen, T.: Glacial--interglacial changes and Holocene variations in Arabian Sea denitrification, Biogeosciences, 15(2), 507–527, doi:10.5194/bg-15-507-2018, 2018.

Giesche, A., Staubwasser, M., Petrie, C. A. and Hodell, D. A.: Indian winter and summer monsoon strength over the 4.2 ka BP event in foraminifer isotope records from the Indus River delta in the Arabian Sea, Clim. Past, 15(1), 73–90, doi:10.5194/cp-15-73-2019, 2019.

Giosan, L., Clift, P. D., Macklin, M. G., Fuller, D. Q., Constantinescu, S., Durcan, J. A., Stevens, T., Duller, G. A. T., Tabrez, A. R., Gangal, K., Adhikari, R., Alizai, A., Filip, F., VanLaningham, S. and Syvitski, J. P. M.: Fluvial landscapes of the Harappan civilization, Proc. Natl. Acad. Sci. U. S. A., 109(26), E1688–E1694, doi:10.1073/pnas.1112743109, 2012.

Giosan, L., Orsi, W. D., Coolen, M., Wuchter, C., Dunlea, A. G., Thirumalai, K., Munoz, S. E., Clift, P. D., Donnelly, J. P., Galy, V. and Fuller, D. Q.: Neoglacial climate anomalies and the Harappan metamorphosis, Clim. Past, 14(11), 1669–1686, doi:10.5194/cp-14-1669-2018, 2018.

Goslin, J., Fruergaard, M., Sander, L., Gałka, M., Menviel, L., Monkenbusch, J., Thibault, N. and Clemmensen, L. B.: Holocene centennial to millennial shifts in North-Atlantic storminess and ocean dynamics, Sci. Rep., 8(1), 12778, doi:10.1038/s41598-018-29949-8, 2018.

Gourlan, A. T., Albarede, F., Achyuthan, H. and Campillo, S.: The marine record of the onset of farming around the Arabian Sea at the dawn of the Bronze Age, The Holocene, 30(6), 878–887, doi:10.1177/0959683620902218, 2020.

Herzschuh, U.: Palaeo-moisture evolution in monsoonal Central Asia during the last 50,000 years, Quat. Sci. Rev., 25(1–2), 163–178, doi:10.1016/j.quascirev.2005.02.006, 2006.

Hou, J., Huang, Y., Zhao, J., Liu, Z., Colman, S. and An, Z.: Large Holocene summer temperature oscillations and impact on the peopling of the northeastern Tibetan Plateau, Geophys. Res. Lett., 43(3), 1323–1330, doi:10.1002/2015GL067317, 2016.

Hunt, K. M. R., Turner, A. G. and Shaffrey, L. C.: The evolution, seasonality and impacts of western disturbances, Q. J. R. Meteorol. Soc., 144(710), 278–290, doi:10.1002/qj.3200, 2018.

Hussain, B. A., Mir, H. and Afzal, M.: Analysis of dust storms frequency over Pakistan during 1961-2000, Pakisan J. Meteorol., 2(3), 2005.

Ivory, S. J. and Lézine, A. M.: Climate and environmental change at the end of the Holocene Humid Period: A pollen record

off Pakistan, Comptes Rendus - Geosci., 341(8–9), 760–769, doi:10.1016/j.crte.2008.12.009, 2009.

Kaniewski, D., Van Campo, E., Guiot, J., Le Burel, S., Otto, T. and Baeteman, C.: Environmental Roots of the Late Bronze Age Crisis, PLoS One, 8(8), 1–10, doi:10.1371/journal.pone.0071004, 2013.

Kaskaoutis, D. G., Rashki, A., Houssos, E. E., Goto, D. and Nastos, P. T.: Extremely high aerosol loading over Arabian Sea during June 2008: The specific role of the atmospheric dynamics and Sistan dust storms, Atmos. Environ., 94, 374–384, doi:10.1016/j.atmosenv.2014.05.012, 2014.

Kaskaoutis, D. G., Rashki, A., Francois, P., Dumka, U. C., Houssos, E. E. and Legrand, M.: Meteorological regimes modulating dust outbreaks in southwest Asia: The role of pressure anomaly and Inter-Tropical Convergence Zone on the 1–3 July 2014 case, Aeolian Res., 18(Supplement C), 83–97, doi:https://doi.org/10.1016/j.aeolia.2015.06.006, 2015.

Klus, A., Prange, M., Varma, V., Bruno Tremblay, L. and Schulz, M.: Abrupt cold events in the North Atlantic Ocean in a transient Holocene simulation, Clim. Past, 14(8), 1165–1178, doi:10.5194/cp-14-1165-2018, 2018.

Kotlia, B. S., Singh, A. K., Joshi, L. M. and Dhaila, B. S.: Precipitation variability in the Indian Central Himalaya during last ca. 4,000 years inferred from a speleothem record: Impact of Indian Summer Monsoon (ISM) and Westerlies, Quat. Int., 371(Supplement C), 244–253, doi:https://doi.org/10.1016/j.quaint.2014.10.066, 2015.

Krishnaswamy, J., Vaidyanathan, S., Rajagopalan, B., Bonell, M., Sankaran, M., Bhalla, R. S. and Badiger, S.: Non-stationary and non-linear influence of ENSO and Indian Ocean Dipole on the variability of Indian monsoon rainfall and extreme rain events, Clim. Dyn., 45(1), 175–184, doi:10.1007/s00382-014-2288-0, 2015.

Laskar, J., Robutel, P., Joutel, F., Gastineau, M., Correia, A. C. M. and Levrard, B.: A long-term numerical solution for the insolation quantities of the Earth, Astron. Astrophys., 428(1), 261–285, doi:10.1051/0004-6361:20041335, 2004.

Lauterbach, S., Witt, R., Plessen, B., Dulski, P., Prasad, S., Mingram, J., Gleixner, G., Hettler-Riedel, S., Stebich, M., Schnetger, B., Schwalb, A. and Schwarz, A.: Climatic imprint of the mid-latitude Westerlies in the Central Tian Shan of Kyrgyzstan and teleconnections to North Atlantic climate variability during the last 6000 years, The Holocene, 24(8), 970–984, doi:10.1177/0959683614534741, 2014.

Lee, J.-Y. and Wang, B.: Future change of global monsoon in the CMIP5, Clim. Dyn., 42(1), 101–119, doi:10.1007/s00382-012-1564-0, 2014.

Leipe, C., Demske, D. and Tarasov, P. E.: A Holocene pollen record from the northwestern Himalayan lake Tso Moriri: Implications for palaeoclimatic and archaeological research, Quat. Int., 348, 93–112, doi:https://doi.org/10.1016/j.quaint.2013.05.005, 2014.

Liu, F. and Feng, Z.: A dramatic climatic transition at ~4000 cal. yr BP and its cultural responses in Chinese cultural domains, The Holocene, 22(10), 1181–1197, doi:10.1177/0959683612441839, 2012.

Lückge, A., Doose-Rolinski, H., Khan, A. ., Schulz, H. and von Rad, U.: Monsoonal variability in the northeastern Arabian Sea during the past 5000years: geochemical evidence from laminated sediments, Palaeogeogr. Palaeoclimatol. Palaeoecol., 167(3), 273–286, doi:10.1016/S0031-0182(00)00241-8, 2001.

Lückge, A., Reinhardt, L., Andruleit, H., Doose-Rolinski, H., von Rad, U., Schulz, H. and Treppke, U.: Formation of varve-

https://doi.org/10.5194/cp-2020-141
Preprint. Discussion started: 17 November 2020

like laminae off Pakistan: decoding 5 years of sedimentation, Geol. Soc. London, Spec. Publ., 195(1), 421–431, doi:10.1144/GSL.SP.2002.195.01.23, 2002.

Madhupratap, M., Kumar, S. P., Bhattathiri, P. M. A., Kumar, M. D., Raghukumar, S., Nair, K. K. C. and Ramaiah, N.: Mechanism of the biological response to winter cooling in the northeastern Arabian Sea, Nature, 384(6609), 549–552, doi:10.1038/384549a0, 1996.

Meyers, P. A. and Ishiwatari, R.: Lacustrine organic geochemistry—an overview of indicators of organic matter sources and diagenesis in lake sediments, Org. Geochem., 20(7), 867–900, doi:10.1016/0146-6380(93)90100-P, 1993.

Mohtadi, M., Prange, M. and Steinke, S.: Palaeoclimatic insights into forcing and response of monsoon rainfall, Nature, 533(7602), 191–199, doi:10.1038/nature17450, 2016.

Moy, C. M., Seltzer, G. O., Rodbell, D. T. and Anderson, D. M.: Variability of El Niño/Southern Oscillation activity at millennial timescales during the Holocene epoch., Nature, 420(6912), 162–5, doi:10.1038/nature01194, 2002.

Munz, P. M., Siccha, M., Lückge, A., Böll, A., Kucera, M. and Schulz, H.: Decadal-resolution record of winter monsoon intensity over the last two millennia from planktic foraminiferal assemblages in the northeastern Arabian Sea, The Holocene, doi:10.1177/0959683615591357, 2015.

Munz, P. M., Lückge, A., Siccha, M., Böll, A., Forke, S., Kucera, M. and Schulz, H.: The Indian winter monsoon and its response to external forcing over the last two and a half centuries, Clim. Dyn., 49(5), 1801–1812, doi:10.1007/s00382-016-3403-1, 2017.

Pease, P. P., Tchakerian, V. P. and Tindale, N. W.: Aerosols over the Arabian Sea: geochemistry and source areas for aeolian desert dust, J. Arid Environ., 39(3), 477–496, doi:10.1006/jare.1997.0368, 1998.

Petrie, C. A. and Bates, J.: `Multi-cropping', Intercropping and Adaptation to Variable Environments in Indus South Asia, J. World Prehistory, 30(2), 81–130, doi:10.1007/s10963-017-9101-z, 2017.

Petrie, C. A., Singh, R. N., Bates, J., Dixit, Y., French, C. A. I., Hodell, D. A., Jones, P. J., Lancelotti, C., Lynam, F., Neogi, S., Pandey, A. K., Parikh, D., Pawar, V., Redhouse, D. I. and Singh, D. P.: Adaptation to Variable Environments, Resilience to Climate Change: Investigating Land, Water and Settlement in Indus Northwest India, Curr. Anthropol., 58(1), 1–30, doi:10.1086/690112, 2017.

Possehl, G. L.: The transformation of the Indus Civilization, J. World Prehistory, 11(4), 425–472, doi:10.1007/BF02220556, 1997.

Prahl, F. G., Muehlhausen, L. A. and Zahnle, D. L.: Further evaluation of long-chain alkenones as indicators of paleoceanographic conditions, Geochim. Cosmochim. Acta, 52(9), 2303–2310, doi:10.1016/0016-7037(88)90132-9, 1988.

Prasad, S. and Enzel, Y.: Holocene paleoclimates of India, Quat. Res., 66(3), 442–453, doi:http://dx.doi.org/10.1016/j.yqres.2006.05.008, 2006.

Prasad, S., Anoop, A., Riedel, N., Sarkar, S., Menzel, P., Basavaiah, N., Krishnan, R., Fuller, D., Plessen, B., Gaye, B., Röhl, U., Wilkes, H., Sachse, D., Sawant, R., Wiesner, M. G. and Stebich, M.: Prolonged monsoon droughts and links to Indo-Pacific warm pool: A Holocene record from Lonar Lake, central India, Earth Planet. Sci. Lett., 391, 171–182,

515 doi:https://doi.org/10.1016/j.epsl.2014.01.043, 2014.

Prasad, S., Marwan, N., Eroglu, D., Goswami, B., Mishra, P. K., Gaye, B., Anoop, A., Basavaiah, N., Stebich, M. and Jehangir, A.: Holocene climate forcings and lacustrine regime shifts in the Indian summer monsoon realm, Earth Surf. Process. Landforms, doi:10.1002/esp.5004, 2020.

von Rad, U., Schulz, H., Khan, A. A., Ansari, M., Berner, U., Čepek, P., Cowie, G., Dietrich, P., Erlenkeuser, H., Geyh, M.,
520 Jennerjahn, T., Lückge, A., Marchig, V., Riech, V., Rösch, H., Schäfer, P., Schulte, S., Sirocko, F., Tahir, M. and Weiss, W.: Sampling the oxygen minimum zone off Pakistan: glacial-interglacial variations of anoxia and productivity (preliminary results, sonne 90 cruise), Mar. Geol., 125(1), 7–19, doi:http://dx.doi.org/10.1016/0025-3227(95)00051-Y, 1995.

von Rad, U., Khan, A. A., Berger, W. H., Rammlmair, D. and Treppke, U.: Varves, turbidites and cycles in upper Holocene sediments (Makran slope, northern Arabian Sea), Geol. Soc. London, Spec. Publ., 195(1), 387–406,
525 doi:10.1144/GSL.SP.2002.195.01.21, 2002.

Rajeevan, M. and Pai, D. S.: On the El Niño-Indian monsoon predictive relationships, Geophys. Res. Lett., 34(4), doi:10.1029/2006GL028916, 2007.

Ramisch, A., Lockot, G., Haberzettl, T., Hartmann, K., Kuhn, G., Lehmkuhl, F., Schimpf, S., Schulte, P., Stauch, G., Wang, R., Wünnemann, B., Yan, D., Zhang, Y. and Diekmann, B.: A persistent northern boundary of Indian Summer Monsoon
530 precipitation over Central Asia during the Holocene., Sci. Rep., 6, 25791, doi:10.1038/srep25791, 2016.

Rao, Z., Wu, Y., Zhu, Z., Jia, G. and Henderson, A.: Is the maximum carbon number of long-chain n-alkanes an indicator of grassland or forest? Evidence from surface soils and modern plants, Chinese Sci. Bull., 56, 1714–1720, doi:10.1007/s11434-011-4418-y, 2011.

Rashki, A., Kaskaoutis, D. G., Rautenbach, C. J. deW., Eriksson, P. G., Qiang, M. and Gupta, P.: Dust storms and their
535 horizontal dust loading in the Sistan region, Iran, Aeolian Res., 5, 51–62, doi:http://dx.doi.org/10.1016/j.aeolia.2011.12.001, 2012.

Rawat, S., Gupta, A. K., Sangode, S. J., Srivastava, P. and Nainwal, H. C.: Late Pleistocene–Holocene vegetation and Indian summer monsoon record from the Lahaul, Northwest Himalaya, India, Quat. Sci. Rev., 114, 167–181, doi:10.1016/j.quascirev.2015.01.032, 2015.

540 Reichart, G. J., Lourens, L. J. and Zachariasse, W. J.: Temporal variability in the northern Arabian Sea oxygen minimum zone (OMZ) during the last 225,000 years, Paleoceanography, 13(6), 607–621, doi:10.1029/98PA02203, 1998.

Rixen, T., Gaye, B. and Emeis, K.-C.: The monsoon, carbon fluxes, and the organic carbon pump in the northern Indian Ocean, Prog. Oceanogr., 175, 24–39, doi:https://doi.org/10.1016/j.pocean.2019.03.001, 2019.

Rommerskirchen, F., Plader, A., Eglinton, G., Chikaraishi, Y. and Rullkötter, J.: Chemotaxonomic significance of distribution
545 and stable carbon isotopic composition of long-chain alkanes and alkan-1-ols in C4 grass waxes, Org. Geochem., 37(10), 1303–1332, doi:10.1016/j.orggeochem.2005.12.013, 2006.

Ruddiman, W. F. and Thomson, J. S.: The case for human causes of increased atmospheric CH4 over the last 5000 years, Quat. Sci. Rev., 20(18), 1769–1777, doi:https://doi.org/10.1016/S0277-3791(01)00067-1, 2001.

https://doi.org/10.5194/cp-2020-141
Preprint. Discussion started: 17 November 2020


Climate of the Past Discussions

Schott, W., von Stackelberg, U., Eckhardt, F. J., Mattiat, B., Peters, J. and Zobel, B.: Geologische Untersuchungen an Sedimenten des indisch-pakistanischen Kontinentalrandes (Arabisches Meer), Geol. Rundschau, 60(1), 264–275, doi:10.1007/BF01820944, 1970.

Schulz, H., Von Rad, U. and Von Stackelberg, U.: Laminated sediments from the oxygen-minimum zone of the northeastern Arabian Sea, Geol. Soc. London, Spec. Publ., 116(116), 185–207, doi:10.1144/GSL.SP.1996.116.01.16, 1996.

Sirocko, F., Sarnthein, M., Lange, H. and Erlenkeuser, H.: Atmospheric summer circulation and coastal upwelling in the Arabian Sea during the Holocene and the last glaciation, Quat. Res., 36(1), 72–93, doi:10.1016/0033-5894(91)90018-Z, 1991.

Sonzogni, C., Bard, E., Rostek, F., Lafont, R., Rosell-Mele, A. and Eglinton, G.: Core-top calibration of the alkenone index vs sea surface temperature in the Indian Ocean, Deep Sea Res. Part II Top. Stud. Oceanogr., 44(6), 1445–1460, doi:10.1016/S0967-0645(97)00010-6, 1997.

Srivastava, P., Agnihotri, R., Sharma, D., Meena, N., Sundriyal, Y. P., Saxena, A., Bhushan, R., Sawlani, R., Banerji, U. S., Sharma, C., Bisht, P., Rana, N. and Jayangondaperumal, R.: 8000-year monsoonal record from Himalaya revealing reinforcement of tropical and global climate systems since mid-Holocene, Sci. Rep., 7(1), 1–10, doi:10.1038/s41598-017-15143-9, 2017.

Staubwasser, M. and Sirocko, F.: On the formation of laminated sediments on the continental margin off Pakistan: the effects of sediment provenance and sediment redistribution, Mar. Geol., 172(1), 43–56, doi:10.1016/S0025-3227(00)00119-5, 2001.

Staubwasser, M., Sirocko, F., Grootes, P. M. and Erlenkeuser, H.: South Asian monsoon climate change and radiocarbon in the Arabian Sea during early and middle Holocene, Paleoceanography, 17(4), doi:10.1029/2000PA000608, 2002.

Staubwasser, M., Sirocko, F., Grootes, P. M. and Segl, M.: Climate change at the 4.2 ka BP termination of the Indus valley civilization and Holocene south Asian monsoon variability, Geophys. Res. Lett., 30(8), doi:10.1029/2002GL016822, 2003.

Stow, D. A. V., Tabrez, A. R. and Prins, M. A.: Quaternary sedimentation on the Makran margin: turbidity current-hemipelagic interaction in an active slope-apron system, Geol. Soc. London, Spec. Publ., 195(1), 219–236, doi:10.1144/GSL.SP.2002.195.01.12, 2002.

Tindale, N. W. and Pease, P. P.: Aerosols over the Arabian Sea: Atmospheric transport pathways and concentrations of dust and sea salt, Deep. Res. Part II Top. Stud. Oceanogr., 46(8–9), 1577–1595, doi:10.1016/S0967-0645(99)00036-3, 1999.

Torrence, C. and Compo, G. P.: A practical guide to wavelet analysis, Bull. Am. Meteorol. Soc., 79(1), 61–78, 1998.

Ummenhofer, C. C., Gupta, A. Sen, Li, Y., Taschetto, A. S. and England, M. H.: Multi-decadal modulation of the El Niño-Indian monsoon relationship by Indian Ocean variability, Environ. Res. Lett., 6(3), 34006, doi:10.1088/1748-9326/6/3/034006, 2011.

Vogts, A., Moossen, H., Rommerskirchen, F. and Rullkötter, J.: Distribution patterns and stable carbon isotopic composition of alkanes and alkan-1-ols from plant waxes of African rain forest and savanna C3 species, Org. Geochem., 40(10), 1037–1054, doi:10.1016/j.orggeochem.2009.07.011, 2009.

Wang, J., Sun, L., Chen, L., Xu, L., Wang, Y. and Wang, X.: The abrupt climate change near 4,400 yr BP on the cultural transition in Yuchisi, China and its global linkage, Sci. Rep., 6, 27723 [online] Available from:

https://doi.org/10.1038/srep27723, 2016.

Wang, P. X., Wang, B., Cheng, H., Fasullo, J., Guo, Z. T., Kiefer, T. and Liu, Z. Y.: The global monsoon across time scales: Mechanisms and outstanding issues, Earth-Science Rev., 174(July 2016), 84–121, doi:10.1016/j.earscirev.2017.07.006, 2017.

Weiss, H., Courty, M.-A., Wetterstrom, W., Guichard, F., Senior, L., Meadow, R. and Curnow, A.: The Genesis and Collapse of Third Millennium North Mesopotamian Civilization, Science (80-.)., 261(5124), 995–1004, doi:10.1126/science.261.5124.995, 1993.

Wright, R. P., Bryson, R. A. and Schuldenrein, J.: Water supply and history: Harappa and the Beas regional survey, Antiquity, 82(315), 37–48, doi:10.1017/S0003598X00096423, 2008.

Yadav, R. K., Rupa Kumar, K. and Rajeevan, M.: Increasing influence of ENSO and decreasing influence of AO/NAO in the recent decades over northwest India winter precipitation, J. Geophys. Res. Atmos., 114(12), 1–12, doi:10.1029/2008JD011318, 2009.

Zhang, X., Jin, L., Chen, J., Lu, H. and Chen, F.: Lagged response of summer precipitation to insolation forcing on the northeastern Tibetan Plateau during the Holocene, Clim. Dyn., 50(9), 3117–3129, doi:10.1007/s00382-017-3784-9, 2018.

Zhao, J., An, C.-B., Huang, Y., Morrill, C. and Chen, F.-H.: Contrasting early Holocene temperature variations between monsoonal East Asia and westerly dominated Central Asia, Quat. Sci. Rev., 178, 14–23, doi:https://doi.org/10.1016/j.quascirev.2017.10.036, 2017.